*Supplemental Information*

*for*

# AN α-HELIX AT THE HORMONE-BINDING SURFACE OF THE INSULIN RECEPTOR FUNCTIONS AS A SIGNALING ELEMENT TO ACTIVATE ITS TYROSINE KINASE*

Jonathan Whittaker, Linda J. Whittaker, Charles T. Roberts, Jr.,
Nelson B. Phillips, Faramarz Ismail-Beigi, Michael C. Lawrence, and Michael A. Weiss

## Table of Contents



## Purpose of Supplement

Methods in Detail provide detailed descriptions of the reagents and experimental procedures employed for mutagenesis, transient expression and evaluation of the variant receptors. Table S1 shows the relative affinities of the variant receptors determined by competitive equilibrium binding assay. Relative affinities of variant receptors with alanine mutations in equivalent positions, determined in prior alanine scanning studies, are shown for comparison (1). Table 2 compares relative affinities of alanine receptor variants for insulin to their relative maximal *in vitro* autophosphorylation response to insulin. Figure S1 shows view of αCT-L1 transdimer interface from Figure 1C in stereo.

## Methods in Detail

*General procedures and materials*—All molecular biological procedures including agarose gel electrophoresis, restriction enzyme digestion, ligation, bacterial transformation and DNA sequencing were performed by standard methods. Oligonucleotides were purchased from Integrated DNA Technologies. Restriction and modifying enzymes were from New England Biolabs. Recombinant human insulin and HPLC-purified mono-iodinated $^{125}$I-Tyr$^{A14}$ insulin were a gift from NovoNordisk A/S. Protease inhibitors were from Roche Molecular Biochemicals. PEAK Rapid cells (293 cells constitutively expressing SV40 large T antigen) were purchased from ATCC. Medium , serum and antibiotics for tissue culture were from Gibco Life Technologies. p-azidophenylalanine (Pap) was from Chem-Impex. The mammalian expression vector pcDNA3.1Zeo+ was from InVitrogen and was modified for C-terminal epitope tagging by subcloning an in-frame oligonucleotide cassette encoding in-frame triple repeats of the FLAG M2 epitope (Asp-Tyr-Lys-Asp-Asp-Asp-Asp-Lys) between the BamHI and XbaI restriction sites (2). Plasmids for expression of a synthetic gene encoding a *B. stearothermophilus* amber suppressor tyrosyl tRNA (pSVB.Yam) and a cDNA encoding a mutated *E. coli* tRNA synthetase specific for p-azidophenylalanine (PAP; pCDNA.FRS) were kindly provided by Drs. Shixin Ye and Thomas P. Sakmar (Rockerfeller University, NY) (3). The cDNA encoding the insulin receptor was as previously described (1) . It was modified for subcloning into the modified expression vector by introduction of a BamHI site encoding an in-frame C-terminal Gly-Ser linker at its 3' end just prior to the stop codon by site-directed mutagenesis (Quikchange, Agilent Technologies) (2) . Monoclonal anti-FLAG M2 IgG was purchased from Sigma-Aldrich. Anti-insulin receptor monoclonal antibody (IgG 83-14) was kindly provided by Dr. K. Siddle (University of Cambridge, U.K.) (4).

*Plasmids*—A cassette containing a triple repeat of the B. stearothermophilus tyrosine amber suppressor tRNA with human the tyrosyl tRNA 5' flanking sequence and 3' terminator sequence, amplified from the plasmid pSVBstYAM (kindly provided by Drs Ye and Sakmar, Rockerfeller University, NY) (3) by PCR was generated between the BamH 1 and EcoR 1 site of the plasmid pTZ19U by SLIC (InFusion: Clontech). This cassette was then excised by digestion with BamH 1 and EcoR 1 sub-cloned into the Mfe1 and Bgl 11 sites of pCDNA3.1zeo (+) (InVitrogen) to produce the plasmid pC3AS. The FLAG-tagged insulin receptor cDNA described above was cloned in to the HindIII and XbaI sites of pC3AS (pC3AS.hIRFl). The *E. coli* tRNA synthetase specific for Pap from pCDNA.FRS (3) was cloned into the HindIII and BamHI sites of pC3AS (pC3AS.FRS). This was further modified by mutation (Quikchange, Agilent Technologies) of the codon for Asp$^{265}$ to that for Arg to enhance recognition of the amber anti-codon by the mutant *E. coli* tRNA synthase specific for

Pap (pC3AS.EnFRS) (5). Amber mutations were introduced into the IR coding sequence of pC3AS.hIRFl by site directed mutagenesis (Quikchange, Agilent Technologies).

*Transient expression of variant receptors*—293PEAK rapid cells (ATCC) were maintained in DMEM 10% FCS containing penicillin and streptomycin, 100μg/ml. For transfection the medium of cells (70-80% confluent) in 10 cm plates was replaced by fresh medium containing PAP 1mM. Three hours later they were co-transfected with amber mutated pC3AS.hIRFl, 10 μg per plate, and pC3AS.EnFRS, 1μg per plate, essentially as previously described (2). Cells were harvested in the absence of direct light by lysis in 0.15M NaCl, 0.1M Tris, pH 8, containing Triton X-100 1% (v/v), glycerol 10% (v/v) and protease inhibitor cocktail (Roche) three days post-transfection when receptor expression was maximal. Lysates were stored at -80 ºC until further manipulation.

*Receptor photo-crosslinking*—All procedures were performed in the absence of direct lighting. Insulin receptors in detergent lysates of transfected cells were enriched by wheat germ agglutinin chromatography by a modification of the method of Hedo *et. al.* (6) , in which Triton X-100, in the wash and elution buffers, was substituted by Igepal 0.01% (v/v). Wheat germ eluate fractions, 2ml, containing insulin receptor were concentrated to 200 μl by centrifugal ultrafiltration (Amicon Ultra 15; NMWL: 30Kda). To evaluate receptor crosslinking to the insulin A-chain, WGA eluates, 40 μl, were incubated overnight at 4 ºC with $^{125}$I-Tyr$^{A14}$ -insulin (240pM) in a volume of 50μl. Binding reactions were then transferred to a pre-blocked white lumitrac 96-well plate (Greiner) and irradiated on ice for 15 secs at a distance of 2 cm from the light source (Mineralight, model LWG-54, UVP Inc., equipped with 254-nm lamp). Crosslinked $^{125}$I-Tyr$^{A14}$-insulin-insulin receptor complexes were resolved by denaturing electrophoresis on 3-8% Tris-acetate gradient gels (Novex, InVitrogen) under reducing conditions and visualized by auto-radiography on Biomax MS X-ray film (Kodak) with a Biomax Transcreen (Kodak) intensifying screen. To visualize receptor crosslinking to the insulin B-chain, WGA eluates were incubated with [biotin aminocaproate$^{B1}$, para-aminophenylalanine$^{A14}$] insulin (100nM) for 30min at 25 ºC prior to UV cross-linking. After resolution of crosslinked samples by reducing SDS-PAGE and transfer to PVDF membranes, photo-adducts were treated with Super-signal enhancer (Thermo-Pierce), probed with streptavidin polyHRP (Thermo-Pierce) and visualized by enhanced chemiluminescence (ECLplus; Thermo-Pierce). To evaluate crosslinking of the intact $^{125}$I-[Tyr$^{A14}$] insulin molecule to the receptor, ligand binding, crosslinking and sample processing were performed identically to the procedure described for A-chain visualization , with the exception that photo-adducts were resolved on non-reducing gels.

For evaluation of insulin receptor α-subunit trans-dimerization, WGA eluates, 40 μl, were incubated with or without recombinant human insulin (100 nM) in a volume of 50μl for 30min at 25 ºC prior to UV crosslinking. Crosslinking, reducing eletrophoresis, and transfer to PDVF membranes were performed as described above. Photo-adducts were probed with anti-insulin receptor antibody (N-20; Santa-Cruz Biotechnology) followed by goat ant-rabbit antibody horse radish peroxidase conjugate (Thermo-Pierce) and visualized by enhanced chemiluminescence (ECLplus; Thermo-Pierce).

*Insulin Binding Assays*- Competitive binding assays with $^{125}$I-Tyr$^{A14}$ -insulin and varying concentrations of unlabeled human recombinant insulin (0-1000nM) were performed on WGA eluates of variant receptors immobilized in micro-titer plates coated with ant-FLAG M2 monoclonal antibody essentially as previously described (2); all experimental manipulations were performed in the absence of direct light. Binding data were analyzed by non-linear regression analysis using a two-site sequential model to obtain $IC_{50}$s for insulin.

*Insulin Receptor Auto-phosphorylation:* Insulin or analog (0-1000nM) is incubated with lectin purified wild type or variant receptor for 60min at 25 ºC. ATP and $Mg^{2+}$ are then added to final concentrations of 2 and 10 mM respectively. After a 30 min incubation, the reaction is terminated by the addition of EDTA. The insulin receptor is then immobilized in microtiter plates coated with anti-receptor MAb 83-7. The phospho-tyrosine content of the immobilized receptor is determined by quantitation of the binding of an Eu-labeled anti-phosphotyrosine antibody (PY20; Perkin-Elmer) by time-resolved fluorescence. EC50, basal and maximal activation are determined by non-linear regression analysis using a 4 parameter logistic model (GraphPad Prism). Concentrations of variant and wild type receptors are normalized prior to assay by determination of relative concentrations in a sandwich ELISA with anti-receptor MAb 83-7 and Eu-labeled anti-receptor MAb 83-14.

*Cellular Studies of Insulin Signaling*. Mouse anti-Akt antibody was from Cell Signaling Technologies (Beverly, MA); rabbit anti-phospho-Akt (pSer493) was from Invitrogen (Carlsbad, CA); mouse Cy5-labeled IgG and rabbit Cy3-labelled IgG secondary antibodies were from GE Healthcare/Amersham. IGF-IR-deficient mouse embryo fibroblast cells (originally provided by Prof. R. Baserga, Thomas Jefferson University, Philadelphia, PA (7)) selectively expressing human receptor isoforms IR-A or IR-B have previously been described (8). Akt phosphorylation as a parameter for activation of the IR signaling pathway was assayed essentially as described previously (8). In brief, cells expressing IR-B were treated with 0.1-10 nM ligand for 5 min and lysed in 1x sodium dodecyl sulphate (SDS) sample buffer without DTT or bromophenol blue and boiled immediately to inhibit protease and phosphatase action. Protein concentration was determined with a detergent-compatible protein assay kit (Bio-Rad). DTT (100 mM) and bromophenol blue (0.1%) were then added. Whole-cell lysates (20 μg) were

subjected to reducing SDS-PAGE on 10% Criterion gels (Bio-Rad) and resolved proteins were transferred to Immobilon FL PVDF membranes (Millipore Corp., Billerica, MA). Blots were probed simultaneously with the Akt and phospho-Akt antibodies (1:2500 and 1:1000 dilutions, respectively), washed 3x with TBS-T buffer, and then probed with a combination of the Cy3 and Cy-5 labeled secondary antisera (1:5000 dilution each). Membranes were washed again 3x with TBS-T, dried, and fluorescent images were captured and quantified using a Fluorchem Q imaging system (Alpha Innotech, San Leandro, CA).

*Rat Assay.* Male Sprague-Dawley rats (mean body mass ~ 0.3 kg) were rendered diabetic by treatment with streptozotocin, as described (9). To test the *in vivo* potency of a representative insulin analog in such diabetic rats to that of wild-type human insulin, protein solutions containing human insulin, KP-insulin, the insulin analog ([$His^{A4}$, $His^{A8}$]-human insulin), or buffer alone (protein-free diluent obtained from Eli Lilly and Co.) were injected subcutaneously, and resulting changes in blood glucose were monitored by serial measurements using a clinical glucometer (Hypoguard Advance Micro-Draw meter). To ensure uniformity of formulation, insulins were each re-purified by reverse-phase HPLC, dried to powder, and dissolved in diluent at the same maximum protein concentration (300 μg/mL); dilutions were made using the above buffer. Rats were injected subcutaneously at time t = 0 with 0.33 to 30 μg insulin in 100 μl of buffer per 0.300 kg rat; the maximal dose corresponds to ca. 100 μg/kg body weight, which corresponds in international units (IU) to 2.9 IU/kg body weight. Blood was obtained from clipped tip of the tail at time t = 0 and every 10 minutes up to 90 min. The efficacy of insulin action to reduce blood glucose level was calculated using the change in blood glucose concentration over time (determined by least-mean squares across the initial region of linear fall) divided by the mass of insulin injected.

**Table S1.** Relative Insulin-Binding Affinities of Variant Holoreceptors

| Variant IR | Relative Affinity (%) | |
|---|---|---|
| | **PAP** | **Ala** |
| **Leu$^{36}$** | 0.4[c] | 19 |
| **Leu$^{37}$** | 0.4[c] | 29 |
| **Leu$^{47}$** | 76 | N.D.[d] |
| **Phe$^{51}$** | 103 | N.D.[d] |
| **Leu$^{62}$** | 11 | 100 |
| **Phe$^{64}$** | 27 | 0.4[c] |
| **Thr$^{704}$** | 0.4[c] | 0.4[c] |
| **Phe$^{714}$** | 118 | 18 |

[a]Results are expressed as relative affinity ($IC_{50}$ Var/$IC_{50}$ WT x100, where $IC_{50}$ is the concentration of insulin that results in 50% inhibition of specific $^{125}$I-Tyr$^{A14}$-insulin binding to the receptor and Var and WT designate variant and wild type receptors respectively).

[b]Data for alanine variants are from ref (1).

[c]These variant IRs exhibited tracer binding that was too low to permit accurate determination of affinity in equilibrium binding assays, and they have thus been arbitrarily assigned a relative affinity of 0.4%.

[d]N.D. indicates that relative affinities of these variants were not determined.

**Table S2.** Hormone-Binding Properties and Signaling by Variant Insulin Receptors

| variant | fold-decrease in insulin affinity[a] | TK activation[b] |
|---|---|---|
| **wild-type IR** | 1 | 100 |
| **F705A** | >250[c] | 8.4 |
| **E706A** | >250[c] | 36.1 |
| **D707A** | 10.1 | 27.9 |
| **Y708A** | 0.8 | 93.8 |
| **L709A** | 4.9 | 8.1 |
| **H710A** | >250[c] | 69.0 |
| **N711A** | >250[c] | 8.9 |
| **V712A** | 0.9 | 97.6 |
| **V713A** | 1.1 | 90.3 |
| **F714A** | 5.4 | 28.1 |
| **V715A** | >250[c] | 42.7 |

[a]Since the majority of Ala substitutions impair binding of insulin, relative changes are expressed as fold-decreased affinities relative to the wild-type hormone-receptor apparent affinity (1/IC50; data from ref. (1)).

[b]TK activation is defined by the maximal extent of autophosphorylation of the variant insulin receptor on binding of wild-type insulin after 30 min at 25 ºC relative to that of wild type receptor; the maximal extent of autophosphorylation was determined by non-linear regression analysis of the dose-response curve.

[c]These variant IRs exhibited tracer binding that was too low to permit accurate determination of affinity in equilibrium binding assays and they have thus been arbitrarily assigned a decrease in affinity of >250-fold .

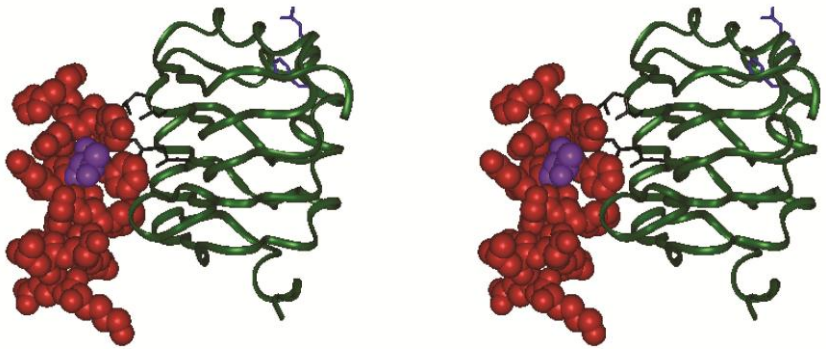

**Figure S1**. Expanded stereo structural views of sites of Pap substitution. Interaction in *trans* between αCT α-helix (*red*) and L1 α-helix (*green*). Side view in which αCT is shown in space-filling representation and L1 as a *ribbon*. L1 side chains pertinent to experimental design are shown: $Leu^{36}$, $Leu^{37}$ and $Leu^{62}$, and $Phe^{64}$ (*black*) and $Arg^{47}$ and $Phe^{51}$ (negative control sites for insulin crosslinking; *blue*). Also shown is negative control site for aporeceptor dimerization ($Thr^{704}$; *magenta*). $Tyr^{714}$, site of a positive control for insulin crosslinking, is not well ordered in the structure. Images are based on Protein Data Bank entry 3LOH.

**Supplementary References**


1. Whittaker J & Whittaker L (2005) Characterization of the functional insulin binding epitopes of the full-length insulin receptor. *J Biol Chem* 280:20932-20936.
2. Whittaker LJ, Hao C, Fu W, & Whittaker J (2008) High affinity insulin binding: Insulin interacts with two receptor ligand binding sites. *Biochemistry* 47:12900-12909.
3. Ye S, Huber T, Vogel R, & Sakmar TP (2009) FTIR analysis of GPCR activation using azido probes. *Nat Chem Biol* 5:397-399.
4. Soos MA, et al. (1986) Monoclonal antibodies reacting with multiple epitopes on the human insulin receptor. *Biochem J* 235:199-208.
5. Takimoto JK, Adams KL, Xiang Z, & Wang L (2009) Improving orthogonal tRNA-synthetase recognition for efficient unnatural amino acid incorporation and application in mammalian cells. *Mol Biosyst* 5:931-934.
6. Hedo JA, Harrison LC, & Roth J (1981) Binding of insulin receptors to lectins: evidence for common carbohydrate determinants on several membrane receptors. *Biochemistry* 20:3385-3393.
7. Sell C, et al. (1993) Simian virus 40 large tumor antigen is unable to transform mouse embryonic fibroblasts lacking type 1 insulin-like growth factor receptor. *Proc Natl Acad Sci USA* 90:11217-11221.
8. Denley A, et al. (2007) Differential activation of insulin receptor substrates 1 and 2 by insulin-like growth factor-activated insulin receptors. *Mol Cell Biol* 27:2569-2577.
9. Saker F, et al. (1998) Glycemia-lowering effect of cobalt chloride in the diabetic rat: Role of decreased gluconeogenesis. *Am J Physiol* 274:E984-E991.